J. Appl. Glycosci.: Advance Publication
doi:10.5458/jag.jag.JAG-2021_0017
Regular Paper (Received December 27, 2021; Accepted February 28, 2022)
J-STAGE Advance Published Date: March 5, 2022

Regular paper

Running title: Acetylated xylan degradation by fungal xylanases

Acetylated xylan degradation by glycoside hydrolase family 10 and 11 xylanases from the white-rot fungus *Phanerochaete chrysosporium*

Keisuke Kojima,[1] Naoki Sunagawa,[1] Yoshihisa Yoshimi,[2] Theodora Tryfona,[2] Masahiro Samejima,[1,3] Paul Dupree,[2] and Kiyohiko Igarashi[1†]

[1]*Department of Biomaterial Sciences, The University of Tokyo* (*1-1-1, Yayoi, Bunkyo-ku, Tokyo 113-8657, Japan*)

[2]*Department of Biochemistry, University of Cambridge* (*Cambridge, Cambridgeshire, CB2 1QW, United Kingdom*)

[3]*Faculty of Engineering*, *Shinshu University* (*4-17-1, Wakasato, Nagano 380-8533, Japan*)

† Corresponding author (Tel. +81-5841-5255, Fax. +81-5841-5273, E-mail: aquarius@mail.ecc.u-tokyo.ac.jp, ORCID ID 0000-0001-5152-7177)

List of abbreviations: Ac, acetyl group; ANTS, 8-aminonaphthalene-1,3,6-trisulfonic acid; Ara*f*, arabinofuranose; AXE, acetyl xylan esterase; BCA, bicinchoninic acid; *Cj*GH10, GH10 xylanase from *Cellvibrio japonicus*; DMSO, dimethyl sulfoxide; DP, degree of polymerization; DW, distilled water; GH, glycoside hydrolase; GlcA, glucuronic acid; MW, molecular weight; *Np*GH11, GH11 xylanase from *Neocallimastix patriciarum*; PACE, polysaccharide analysis using carbohydrate gel electrophoresis; *Pc*Xyn10A, GH10 xylanase from *Phanerochaete chrysosporium*; *Pc*Xyn11B, GH11 xylanase from *P. chrysosporium*; X_2, xylobiose; X_3, xylotriose; X_4, xylotetraose; X_5, xylopentaose; X_6, xylohexaose.

Abstract

Endo-type xylanases are key enzymes in microbial xylanolytic systems, and xylanases belonging to glycoside hydrolase (GH) families 10 or 11 are the major enzymes degrading xylan in nature. These enzymes have typically been characterized using xylan prepared by alkaline extraction, which removes acetyl sidechains from the substrate, and thus the effect of acetyl groups on xylan degradation remains unclear. Here, we compare the ability of GH10 and 11 xylanases, *Pc*Xyn10A and *Pc*Xyn11B, from the white-rot basidiomycete *Phanerochaete chrysosporium* to degrade acetylated and deacetylated xylan from various plants. Product quantification revealed that *Pc*Xyn10A effectively degraded both acetylated xylan extracted from *Arabidopsis thaliana* and the deacetylated xylan obtained by alkaline treatment, generating xylooligosaccharides. In contrast, *Pc*Xyn11B showed limited activity towards acetyl xylan, but showed significantly increased activity after deacetylation of the xylan. Polysaccharide analysis using carbohydrate gel electrophoresis showed that *Pc*Xyn11B generated a broad range of products from native acetylated xylans extracted from birch wood and rice straw, including large residual xylooligosaccharides, while non-acetylated xylan from Japanese cedar was readily degraded into xylooligosaccharides. These results suggest that the degradability of native xylan by GH11 xylanases is highly dependent on the extent of acetyl group substitution. Analysis of 31 fungal genomes in the Carbohydrate-Active enZymes database indicated that the presence of GH11 xylanases is correlated to that of carbohydrate esterase family 1 acetyl xylan esterases (AXEs), while this is not the case for GH10 xylanases. These findings may imply co-evolution of GH11 xylanases and CE1 AXEs.

Keywords: Xylanase; glycoside hydrolase; acetylated xylan; *Phanerochaete chrysosporium*; biomass utilization

INTRODUCTION

Plant cell walls are composed of three main components, i.e., cellulose, hemicellulose and lignin, and enzymatic saccharification is a mild and effective way to utilize cellulose and hemicellulose as a source of biofuel and bio-based chemicals that can replace fossil resources. Recently, it was shown that the degradation of hemicellulose is the bottleneck in enzymatic saccharification of plant biomass[1)], and thus degradation of hemicellulose is as important as that of cellulose. In plant cell walls, hemicelluloses interact strongly with other components. For instance, xylan, a common hemicellulose of terrestrial plants, can be on the surface of cellulose[2)3)] and can also be chemically linked to lignin to form lignin-carbohydrate complexes (LCCs)[4)5)].

The main chain of xylan consists of β-1,4-linked xylose residues, whereas the side chains, such as glucuronic acid (GlcA), arabinofuranose (Ara*f*) and acetyl groups (Ac), differ among different plant species. Acetylation in hardwood secondary cell walls is largely on alternate xylose residues and can substitute O2 and/or O3 of xylose residues with a degree of acetylation over 0.5[6)]. In gymnosperm, softwoods, xylan is not acetylated, while there are moderate levels of acetylation in grasses[7)]. In nature, xylan is degraded by a series of enzymes produced by fungi and bacteria[8)9)]. Main chain degradation is performed by endo-xylanases (Xyn, EC 3.2.1.8), which can degrade xylan polymer into xylooligosaccharides, and then β-xylosidase (EC 3.2.1.37) produces xylose monomer from the xylooligosaccharides, with an aid of accessary enzymes. GlcA, Ara*f* and Ac are removed by xylan α-1,2-glucuronosidase (EC 3.2.1.131), α-L-

arabinofuranosidase (EC 3.2.1.55), and acetyl xylan esterase (AXE, EC 3.2.1.72), respectively.

Most of fungal xylanases, the key enzymes of the xylan degradation system, are classified into glycoside hydrolase (GH) families 10, 11 and 30 in the Carbohydrate-Active enZymes (CAZy) database (http://www.cazy.org/)[10]. GH10 and 11 xylanases, the major enzymes among wood-decay fungi[11], are reported to show no distinct substate preferences, i.e., both enzymes are capable of degrading various xylooligosaccharides and non-acetylated xylan, based on their reaction properties and crystal structures[12)13)14)15)16]. However, although those substrates lack acetyl groups, native xylans from plants other than gymnosperm are modified with acetyl groups, and the products of degradation of acetylated xylan by GH10 and 11 xylanases are quite diverse[9]. Thus, the substrate specificity of xylanases towards acetylated xylan remains unclear. The aim of this work was to investigate the substrate preferences of GH10 and 11 xylanases from the basidiomycete *Phanerochaete chrysosporium*[17] (*Pc*Xyn10A and *Pc*Xyn11B) by means of time course experiments and analysis of the final products generated from native acetylated xylan, deacetylated xylan obtained by alkaline treatment and non-acetylated xylan.

MATERIALS AND METHODS

Cloning. *P. chrysosporium* strain K-3 was grown on Kremer and Wood medium[18] containing 2 % Avicel (Sigma-Aldrich, MA, USA) as the sole carbon source. Total RNA was extracted from approximately 100 mg of frozen mycelial powder using RNeasy (QIAGEN, Limburg, Netherlands), and mRNA was purified using Oligo dT Latex (Takara Bio, Shiga, Japan), as per the instructions. cDNA from mRNA was synthesized using a GeneRacer kit (Invitrogen, MA, USA). The primers for amplification from cDNA were designed based on the genomic sequences of *P. chrysosporium* as shown in Table S1. To determine and obtain the full-length sequences of *pcxyn10a*, the primers FW_PcXyn10A_5'UTR2 and RV_PcXyn10A_3'UTR2 were used. For *pcxyn11b*, FW_PcXyn11B_5'UTR and RV_PcXyn11B_3'UTR were used. All PCR products were cloned using a Zero Blunt TOPO PCR Cloning kit for Sequencing (Thermo Fisher Science, MA, USA). The amino acid sequences of *Pc*Xyn10A and *Pc*Xyn11B were analyzed by SignalP 5.0[19] and Pfam 31.0[20] to identify signal peptides and domain structures, respectively. pPICZα plasmid with Ste13 cleavage sites removed and *pcxyn10a* or *pcxyn11b* were fused using an In-Fusion HD cloning Kit (Takara Bio). Each sequence was located between Kex2 and Xba I sites in the pPICZα plasmid. After transformation of the methylotrophic *Pichia pastoris* strain KM71H by electroporation, transformants were selected using Zeocin according to the manual.

Enzyme preparations. Recombinant proteins were obtained by using a 5-L jar fermenter (TSC-M5L; Takasugi Seisakusho, Tokyo, Japan) with methanol feed according to the reported method[21][22]. After protein production was finished, each medium was collected by centrifugation at 5,000 × G for 30 min.

The collected medium was passed through a 100 kDa filter and concentrated using a 10 kDa filter (Millipore, MA, USA). The concentrate was purified on a hydrophobic interaction column (TOYOPEARL Phenyl 650M, TOSOH, Tokyo, Japan). After equilibration with 50 mM sodium acetate buffer (pH 5.0) containing 1 M ammonium sulfate (Wako, Osaka, Japan), enzymes were eluted with 50 mM sodium acetate buffer (pH 5.0). An anion-exchange column (TOYOPEARL 650S, TOSOH) was used for further purification. After equilibration with 50 mM Tris-HCl buffer (pH 7.0), the enzymes were eluted with 50 mM Tris-HCl buffer (pH 7.0) containing 1 M NaCl. To confirm purity, 12 % SDS-PAGE was performed.

GH10 xylanase from *Cellvibrio japonicus* (*Cj*GH10)[23] was a kind gift from Professor Harry Gilbert (York University) and GH11 xylanase from *Neocallimastix patriciarum* (*Np*GH11)[15] was purchased from Megazyme (Wicklow, Ireland).

Crude protein was quantified using the Bradford Protein Assay (Bio-Rad, CA USA) with bovine serum albumin as a standard. Purified enzymes were quantified with a NanoDrop2000 (Thermo Fisher Scientific).

Preparation of native xylans from various plants. Acetylated xylan from *Arabidopsis thaliana* was extracted based on the method reported by Busse-Wicher *et al*.[6]. Approximately 100 mg of alcohol-insoluble residue from stems of *A. thaliana*, prepared as previously described[24], was depectinated in 0.5 (w/v) % ammonium oxalate at 85 ℃ for 2 h. The sample was then washed with water and delignified in 11 % peracetic acid at 85 ℃ for 30 min. Finally, acetylated xylan was extracted from holocellulose with dimethyl sulfoxide (DMSO), and the solvent was changed to distilled water (DW) using a PD-10 column (GE Healthcare, Il, USA). For analysis of the sugar content, TFA

hydrolysis of this acetylated xylan and high-pressure ion chromatography using Dionex (Dionex, CA, USA) were conducted.

Native xylans were also extracted from birch wood, Japanese cedar, and rice straw. Wood blocks and rice straw were dried, milled and meshed as described previously[1]. Samples were depectinated as described above and delignified according to Klaudiz[25][26]. One g of powder sample, 0.8 g of $NaClO_2$ and 150 mg of acetic acid (Wako) were mixed with 11 mL of DW and incubated at 37 ℃ for 40 h. Acetylated xylans were extracted from birch wood and rice straw with DMSO, and non-acetylated xylan was extracted from Japanese cedar with 4 M KOH. After extraction, the solvents were replaced with DW as described above.

To estimate the ratio of xylan components, ^{1}H-NMR spectra were acquired at 20 ℃ on a 500 MHz spectrometer (JNM-ECA500II, JEOL, Tokyo, Japan). For NMR, non-acetylated xylan from Japanese cedar was purified by adding saturated $Ba(OH)_2$ (Wako) solution to precipitate mannan. Approximately 20 mg of each substrate was dissolved in 1 mL of D_2O (Sigma-Aldrich) and centrifuged to remove solids. The results were analyzed by means of delta software (version 6.0.0, JEOL). The ^{1}H NMR assignments were conducted by comparison with reported NMR spectral data for acetylated xylans from dicots[27][28][29], acetylated xylans from grasses[7][30] and non-acetylated xylan from softwood[31]. The peak of xylose residue without side chain (Free Xyl: 4.33 ppm), those of GlcA-substituted xylose residue (GlcA-Xyl: 4.96 and 5.15 ppm), those of acetylated xylose residue (Ac-Xyl: 4.42, 4.55, 4.96 and 5.03ppm), that of Ara*f*-substituted xylose residue (Ara*f*-Xyl: 5.25 ppm) were assigned and integrated. The ratio of xylan components was estimated from the peak area ratios (Table 1).

Time course study. The increase in the amount of reducing ends was measured by means of the bicinchoninic acid (BCA, TCI, Tokyo, Japan) method[32] with few modifications. The reaction solution consisted of 4 nM purified enzyme, 1.67 μM acetylated xylan from *A. thaliana*, and 50 mM ammonium acetate buffer (pH 5.0). The reaction was stopped at 0, 5, 10, 30, and 60 min by adding alkali solution in BCA methods. The ratio of each sample, solution A (5.65 mM BCA, 512 mM and 288 mM $NaHCO_3$) and solution B (7.82 mM $CuSO_4 \cdot 5H_2O$ and 12.0 mM L-serine) was 1: 2: 2. Those mixed samples were heated at 80 ℃ for 30 min and cooled on ice. Finally, the absorbance at 560 nm was determined and the concentration of produced reducing ends was calculated based on a xylose standard curve. Results were fit to the following first-order equation using R (version 3.6.3),

$$y = S\left(1 - e^{-t/\tau}\right)$$

where y and t are the concentration of released reducing ends (μM) and the reaction time (h), respectively, S is the concentration of degradable regions of each substrate (μM) by different xylanases. τ is the time constant (h).

Alkaline treatment of the same acetylated xylan was conducted for deacetylation to prepare deacetylated xylan polymer at the same concentration as the acetylated xylan polymer. First, 4 M NaOH was added to acetylated xylan solution and the mixture was incubated at room temperature for 20 min. Then, 1 M HCl was added for neutralization. The ratio of acetylated xylan solution, NaOH and HCl was 200: 5: 20.

Polysaccharide analysis using carbohydrate gel electrophoresis. For analysis of the final products after digestion of acetylated xylan from *A. thaliana*, polysaccharide analysis using carbohydrate gel electrophoresis (PACE)[33] with 10 w/v % polyacrylamide gels was adopted. Gels were prepared as described by Bromley *et al.*[34]

191 with modifications in the composition of gels. One 10 w/v % polyacrylamide gel
192 consisted of 20.4 mL of DW, 3 mL of 1 M tris(hydroxymethyl)aminomethane-base
193 borate (pH 8.2), 8.4 mL of 40 % polyacrylamide (29:1; acrylamide/bis), 24 µL of N, N,
194 N', N'-tetramethylethylenediamine and 180 µL of 10 % ammonium persulfate. The
195 reaction solution was the same as used for the time course study and was incubated at
196 30 ℃ for 24 h. After digestion, samples were dried using a Speed-Vac (Thermo Fisher
197 Scientific) and labelled overnight with 8-aminonaphthalene-1,3,6-trisulfonic acid
198 (ANTS) as described by Bromley *et al*[34]. ANTS-Labelled samples were dried using a
199 Speed-Vac and resuspended in 3 M urea as PACE samples. Standards, a mixture of
200 xylooligosaccharides (Megazyme), were also labelled. Electrophoresis of *A. thaliana*
201 samples was conducted using a Hofer SE660 (Hoefer, MA, USA) at 1,000 V for 45
202 min. Visualization of PACE gels was carried as described by Bromley *et al*.[34].
203 For comparison of the degradation of various xylans, large custom glass plates
204 (160 mm width and 300 mm height) and equipment for 10 % PACE gels were obtained
205 from Nihon Eido (Tokyo, Japan). Composition of the gel was the same as above.
206 Electrophoresis was conducted at 1,000 V for 1 h. PACE gels were visualized in a box
207 covered with aluminum foil, using an LED lighting device (Optocode, Tokyo, Japan)
208 emitting at 365 nm. Image J (version 1.53) was used for analysis of bands intensities.
209
210 ***Correlation analysis between xylanases and AXEs.*** The correlation coefficients, *r*,
211 between the numbers of enzymes were calculated as the following equation:

212 $$r = \frac{cov(x, y)}{\sigma_x \times \sigma_y}$$

213 where cov(x, y), σ_x, and σ_y mean the covariance between *x* and *y*, the standard deviation
214 of *x* and that of *y*. *x* and *y* were the numbers of each enzymes based on previous

215 research[35]. For the calculation of those between the existence of enzymes, the numbers
216 were standardized: absence is zero and existence is one.

RESULTS and DISCUSSION

Cloning and preparation of* Pc*Xyn10A and* Pc*Xyn11B. *P. chrysosporium* has 6 genes encoding GH10 xylanase and one gene encoding GH11 xylanase[35]. Previous reports confirmed that *P. chrysosporium* secrets two GH10 xylanases, *Pc*Xyn10A and *Pc*Xyn10C, during culture using only cellulose or cellulose and xylan as carbon resources and that *Pc*Xyn10A is more constantly expressed than *Pc*Xyn10C. Therefore, *Pc*Xyn10A was selected as the representative GH10 xylanase for *P. chrysosporium* in this paper. Cloning of *pcxyn10a* and *pcxyn11b* was successful (Fig. S1). *Pc*Xyn10A and *Pc*Xyn11B consisted of 389 and 271 amino acids, respectively, and lacked any signal peptide according to SignalP 5.0[19] (Fig. 1). The amino acid sequences were analyzed by HMMER[36], which indicated the presence of a CBM1 domain at the N-terminal and C-terminal ends of *Pc*Xyn10A and *Pc*Xyn11B, respectively.

Recombinant *Pc*Xyn10A and *Pc*Xyn11B were produced in a jar-fermenter and purified by ultrafiltration and column chromatography. Purity was examined by SDS-PAGE, as shown in Fig. S2, and the purest samples were used for activity testing. Since both proteins contain CBM1 and a linker, the molecular weights are higher than those of the catalytic domain alone. The theoretical molecular weight of *Pc*Xyn10A is 42,000 and that of *Pc*Xyn11B is 29,000, whereas the observed values were around 45,000 and 37,000, respectively, in SDS-PAGE. Larger molecular weight of *Pc*Xyn11B in appearance is consistent with previous results[37][38] and the large difference between of the two values for *Pc*Xyn11B is due to glycosylation.

Analysis of the average DP after digestion of acetylated xylan. The results of digestion of acetylated xylan extracted from *A. thaliana*, in which more than half of the xylose residues are acetylated[6] (Tables 1), is shown in Fig. 2. To compare xylanases from *P.*

chrysosporium and well-characterized xylanases, *Cj*GH10 and *Np*GH11 without CBMs were also tested, because *Cj*GH10 and *Np*GH11 were known as efficient enzymes in GH10 and GH11 xylanases, as additive enzyme to commercial enzymes cocktails for biomass saccharification in the previous report[1]. GH10 xylanases degrade even this densely acetylated xylan into oligosaccharides. Although the τ-values, the time constant, of *Pc*Xyn10A (0.21 ± 0.02 h) and *Cj*GH10 (0.12 ± 0.03 h) were somewhat different, the *S*-values, the concentration of degradable regions of the substrate, were similar at 28.0 ± 0.9 and 24.6 ± 1.6 μM, respectively, indicating that both enzymes have similar ability to degrade acetylated xylan (Table 2). Based on the *S*-values, the average DP after reaction was estimated as 9.6 and 11 for *Pc*Xyn10A and *Cj*GH10, respectively. Since the DP of xylan polymer is approximately 150[39], GH10 xylanases cleaved one molecule of acetylated xylan approximately 14 times. After removal of acetyl groups by alkaline treatment, the *S*-values of *Pc*Xyn10A and *Cj*GH10 were 47.3 ± 1.2 and 37.4 ± 1.2 μM, respectively, being 1.7 and 1.5 times larger than the values for acetylated xylan. Compared among GH10 xylanases, *Cj*GH10 showed the smaller values of τ and *S*, suggesting that *Cj*GH10 can bind substrates more selectively than *Pc*Xyn10A.

In contrast, GH11 xylanases attacked acetylated xylan from *A. thaliana* much less effectively than did GH10 xylanases, and the *S*-values were 5.2 ± 0.8 μM for *Pc*Xyn11B and 7.8 ± 0.2 μM for *Np*GH11. The average DPs after digestion were 45 and 32, respectively, indicating that only 3.3 and 4.7 cleavages occurred per acetylated xylan molecule. However, after deacetylation, the *S*-values of *Pc*Xyn11B and *Np*GH11 were 38.0 ± 2.2 and 32.6 ± 0.4 μM, respectively, being 7.3 and 4.2 times higher than those for acetylated xylan. Comparing all xylanases tested, *Np*GH11 showed the smallest value of τ for deacetylated xylan, suggesting that *Np*GH11 may have evolved to act specifically on deacetylated xylan.

It was reported that acetylation contributes to the resistance of xylan to enzymatic degradation[40], and our results show that acetylation has a greater negative effect on GH11 xylanases than on GH10 xylanases. As shown in Table 1, since half of xylose residues are acetylated in *A. thaliana* xylan, the probability of three connected free xylose will appear in every 8 residues. However, in the present results, GH11 xylanases, which require three free xylose residues[16], showed less activity than expected, indicating the side chain of acetylated xylan from *A. thaliana* should be regular, which is unfavorable to GH11 activity. Moreover, assuming that the acetyl group modification is every other xylose residue, the degradation of GH10 xylanases did not complete, suggesting that the position of the acetyl group substitutions is important for GH10 to accommodate acetylated xylan. Further analysis of crystal structures with acetylated xylan is necessary to reveal the details.

Analysis of final products by PACE. A time course study revealed that longer xylooligosaccharides remained undegraded even after prolonged incubation, especially with GH11 xylanases, and the distribution of final products was still unclear. Therefore, 10 % PACE gel was used to separate oligosaccharides with various DPs. As shown in Fig. 3, xylan and longer xylooligosaccharides appeared as a smear at the upper side of the gels, while several peaks appeared after hydrolysis. *Pc*Xyn10A degraded acetylated xylan mainly into xylooligosaccharides with DP<10, which is consistent with the value estimated from reducing-sugar analysis. After deacetylation, as expected, *Pc*Xyn10A xylanases produced smaller oligosaccharides, again in agreement with the biochemical results.

In contrast to *Pc*Xyn10A, *Pc*Xyn11B degraded acetylated xylan mainly into large compounds which remained at the upper part of the gel, suggesting that the action

of *Pc*Xyn11B is clearly blocked by acetyl group substitution. However, after deacetylation, *Pc*Xyn11B produced smaller oligosaccharides and the final products of deacetylated xylan had a DP of 6 or less (Fig. 3B). Although more data is needed to identify final products completely, it was confirmed that acetylated xylan from *A. thaliana* is not a favorable substrate for *Pc*Xyn11B, in contrast to *Pc*Xyn10A.

Comparison of degradation of various xylans. To compare the degradation of various native xylans by *Pc*Xyn10A and *Pc*Xyn11B, we focused on two acetylated xylans from birch wood and rice straw and one non-acetylated xylan from Japanese cedar. As summarized in Table 1, acetylated xylan from birch wood consisted of 45.5 ± 1.2 % free xylose residues, 51.1 ± 0.8 % acetylated xylose residues and 6.6 ± 0.9 % GlcA-substituted xylose residues. While the acetylation ratio is similar to that of acetylated xylan from *A. thaliana*[6], the ratio of GlcA/Xyl is slightly smaller[34]. Acetylated xylan from rice straw consisted of 64.5 ± 0.7 % free xylose residues, 25.9 ± 0.8 % acetylated xylose residues, 0.8 ± 0.1 % GlcA-substituted xylose residues and 8.7 ± 0.3 % Ara*f* -substituted xylose residues. It has been reported that acetylated xylans from grasses contain 60 - 80 % free xylose residues, while other xylose residues are substituted mostly with acetyl groups, as well as Ara*f* and GlcA in that order[7]. Non-acetylated xylan from Japanese cedar consisted of 74.8 ± 0.4 % free xylose residues, 17.4 ± 0.2 % GlcA-substituted xylose residues and 7.8 ± 0.6 % Ara*f*-substituted xylose residues. The ratios of GlcA/Xyl and Ara*f*/Xyl are approximately 1/6 and 1/13, respectively. Two major motifs of non-acetylated xylan from softwood were previously identified as α-L-arabinofuranosyl- α-D-glucuronyl xylohexaose and α-D-glucuronyl xylohexaose[41], and small amounts of other motifs are also present[42]. These values are similar to those of non-acetylated xylan from softwoods.

317 The results of digestion of the three selected xylans by *Pc*Xyn10A and
318 *Pc*Xyn11B are shown in Fig. 4. *Pc*Xyn10A degraded acetylated xylan from birch wood
319 similarly to acetylated xylan from *A. thaliana*. The pattern of degradation products of
320 acetylated xylan from rice straw was similar to that of acetylated xylan from birch wood
321 (Fig. 4A), whereas their components are different. *Pc*Xyn10A produced smaller
322 oligosaccharides from acetylated xylan of rice straw as compared with those from
323 acetylated xylan of birch wood due to less acetylation of rice straw xylan. The peak
324 intensities were quantified by Image J as shown in Fig. 4B. The final products of
325 acetylated xylans from both plants were mainly oligosaccharides with DP < 15, as in the
326 case of *A. thaliana*. The results for *Pc*Xyn11B are also shown in Fig. 4. *Pc*Xyn11B did
327 not degraded acetylated xylans as well as *Pc*Xyn10A, as was the case for the acetyl
328 xylan from *A. thaliana*. However, non-acetylated xylan from Japanese cedar was
329 degraded well not only by *Pc*Xyn10A, but also by *Pc*Xyn11B. These results are
330 consistent with the idea that acetyl group substitution can interfere with the action of
331 GH11 enzymes, but not GH10 enzymes much.
332
333 ***The evolutionary relationship between fungal xylanases and AXEs.*** Fig. 5 shows the
334 putative relationship between fungal evolution and the numbers of GH10, GH11
335 xylanases and CE1 enzymes which are classified as AXEs[6], based on previous
336 research[35]. To examine the relationships of these enzymes in fungal xylan degradation
337 systems, the correlation coefficients between the numbers of enzymes were calculated
338 (Table 3). The correlation between numbers of GH10 and GH11 enzymes is weak
339 (correlation coefficient less than 0.5), while numbers of CE1 enzymes show high
340 correlation coefficients of approximately 0.7 with the numbers of both GH10 and GH11

341 enzymes. These results suggest that fungi possessing a large number of xylanases also
342 tend to possess a large number of AXEs.
343 Furthermore, the correlation coefficient between the existence of GH10 and CE1
344 enzymes is low, under 0.4, while that between the existence of GH11 and CE1 enzymes
345 is approximately 0.6. Nine of 10 fungi having GH11 xylanase genes have CE1 genes,
346 though only 14 fungi carry CE1 genes among the 31 fungi considered here. These
347 results suggest that coevolution of these families' enzymes may have occurred. This
348 seems plausible because GH11 enzymes would require deacetylation by CE1 AXEs in
349 order to work well in hydrolyzing xylan.
350 It is worth noting that acetyl group(s) should be removed even after degradation
351 by GH10 enzymes in order to facilitate the reaction of glycosidases. Thus, there may be
352 so-far-unidentified AXEs associated with GH10. In evolutionary terms, it seems that
353 GH10 xylanases appeared much earlier than GH11 xylanases, and fungi and molds may
354 have acquired GH11 and CE1 concomitantly from the Carboniferous period to the
355 Permian period, when gymnosperms and angiosperms appeared. Brown-rot fungi tend
356 to have fewer GH11 and CE1 enzymes in their genome, which is reasonable because
357 these fungi prefer softwood to hardwood. Thus, the evolution of plant species having
358 acetyl side chains on xylan may have led to the appearance of relevant enzymes in
359 fungal xylan-degrading systems.
360 We believe the present findings will be helpful not only in understanding how
361 plant biomass is degraded in nature, but also in improving the efficiency of human
362 utilization of cellulosic biomass.
363

Acknowledgement

We wish to thank Professor Harry Gilbert for the kind gift of *Cj*GH10. This work was supported in part by a Grant-in-Aid for Scientific Research (B) 19H03013 (to K.I.), a Grant-in-Aid for Early-Career Scientists 19K15884 (to N.S.) from the Japan Society for the Promotion of Science (JSPS) and a Grant-in-Aid for Innovative Areas 18H05494 (to K.I.) from the Japanese Ministry of Education, Culture, Sports, and Technology (MEXT).

REFERENCES

1) K. Sakuragi, K. Igarashi, and M. Samejima: Application of ammonia pretreatment to enable enzymatic hydrolysis of hardwood biomass. *Polym. Degrad. Stab.*, **148**, 19–25 (2018).

2) T. J. Simmons, J. C. Mortimer, O. D. Bernardinelli, A. C. Pöppler, S. P. Brown, E. R. DeAzevedo, R. Dupree, and P. Dupree: Folding of xylan onto cellulose fibrils in plant cell walls revealed by solid-state NMR. *Nat. Commun.*, **7**, 1–9 (2016).

3) T. Wang, H. Yang, J. D. Kubicki, and M. Hong: Cellulose structural polymorphism in plant primary cell walls investigated by high-field 2D solid-state NMR spectroscopy and density functional theory calculations. *Biomacromolecules*, **17**, 2210–2222 (2016).

4) N. Takahashi, and T. Koshijima: Ester linkages between lignin and glucuronoxylan in a lignin-carbohydrate complex from beech (*Fagus crenata*) wood. *Wood Sci. Technol.*, **22**, 231–241 (1988).

5) X. Du, M. Pérez-Boada, C. Fernández, J. Rencoret, J. C. del Río, J. Jiménez-Barbero, J. Li, A. Gutiérrez, and A. T. Martínez: Analysis of lignin–carbohydrate and lignin–lignin linkages after hydrolase treatment of xylan–lignin, glucomannan–lignin and glucan–lignin complexes from spruce wood. *Planta*, **239**, 1079–1090 (2014).

6) M. Busse-Wicher, T. C. F. Gomes, T. Tryfona, N. Nikolovski, K. Stott, N. J. Grantham, D. N. Bolam, M. S. Skaf, and P. Dupree: The pattern of xylan acetylation suggests xylan may interact with cellulose microfibrils as a twofold helical screw in the secondary plant cell wall of *Arabidopsis thaliana*. *Plant J.*, **79**, 492–506 (2014).

7) D. Morais de Carvalho, A. M. Abad, D. V. Evtuguin, J. L. Colodette, M. E. Lindström, F. Vilaplana, and O. Sevastyanova: Isolation and characterization of acetylated glucuronoarabinoxylan from sugarcane bagasse and straw. *Carbohydr. Polym.*, **156**, 223–234 (2017).

8) P. Biely, S. Singh, and V. Puchart: Towards enzymatic breakdown of complex plant xylan structures: state of the art. *Biotechnol. Adv.*, **34**, 1260–1274 (2016).

9) P. Biely, M. Cziszárová, I. Uhliariková, J. W. Agger, X. L. Li, V. G. H. Eijsink, and B. Westereng: Mode of action of acetylxylan esterases on acetyl glucuronoxylan and acetylated oligosaccharides generated by a GH10 endoxylanase. *Biochim. Biophys. Acta - Gen. Subj.*, **1830**, 5075–5086 (2013).

10) V. Lombard, H. Golaconda Ramulu, E. Drula, P. M. Coutinho, and B. Henrissat: The carbohydrate-active enzymes database (CAZy) in 2013. *Nucleic Acids Res.*, **42**, 490–495 (2014).

11) C. Hori, J. Gaskell, K. Igarashi, M. Samejima, D. Hibbett, B. Henrissat, and D. Cullen: Genomewide analysis of polysaccharides degrading enzymes in 11 white- and brown-rot Polyporales provides insight into mechanisms of wood decay. *Mycologia*, **105**, 1412–1427 (2013).

12) P. Biely, M. Vršanská, M. Tenkanen, and D. Kluepfel: Endo-β-1,4-xylanase families: differences in catalytic properties. *J. Biotechnol.*, **57**, 151–166 (1997).

13) G. Pell, E. J. Taylor, T. M. Gloster, J. P. Turkenburg, C. M. G. A. Fontes, L. M. A. Ferreira, T. Nagy, S. J. Clark, G. J. Davies, and H. J. Gilbert: The mechanisms by which family 10 glycoside hydrolases bind decorated substrates. *J. Biol. Chem.*, **279**, 9597–9605 (2004).

14) Z. Fujimoto, S. Kaneko, A. Kuno, H. Kobayashi, I. Kusakabe, and H. Mizuno: Crystal structures of decorated xylooligosaccharides bound to a family 10

xylanase from *Streptomyces olivaceoviridis* E-86. *J. Biol. Chem.*, **279**, 9606–9614 (2004).

15) M. Vardakou, C. Dumon, J. W. Murray, P. Christakopoulos, D. P. Weiner, N. Juge, R. J. Lewis, H. J. Gilbert, and J. E. Flint: Understanding the structural basis for substrate and inhibitor recognition in Eukaryotic GH11 xylanases. *J. Mol. Biol.*, **375**, 1293–1305 (2008).

16) Z. Fujimoto, N. Kishine, K. Teramoto, S. Tsutsui, and S. Kaneko: Structure-based substrate specificity analysis of GH11 xylanase from *Streptomyces olivaceoviridis* E-86. *Appl. Microbiol. Biotechnol.*, **105**, 1943–1952 (2021).

17) D. Martinez, L. F. Larrondo, N. Putnam, M. D. Sollewijn Gelpke, K. Huang, J. Chapman, K. G. Helfenbein, P. Ramaiya, J. C. Detter, F. Larimer, P. M. Coutinho, B. Henrissat, R. Berka, D. Cullen, and D. Rokhsar: Genome sequence of the lignocellulose degrading fungus *Phanerochaete chrysosporium* strain RP78. *Nat. Biotechnol.*, **22**, 695–700 (2004).

18) S. M. Kremer, and P. M. Wood: Evidence that cellobiose oxidase from *Phanerochaete chrysosporium* is primarily an Fe(III) reductas: kinetic comparison with neutrophil NADPH oxidase and yeast flavocytochrome b_2. *Eur. J. Biochem.*, **205**, 133–138 (1992).

19) J. J. Almagro Armenteros, K. D. Tsirigos, C. K. Sønderby, T. N. Petersen, O. Winther, S. Brunak, G. von Heijne, and H. Nielsen: SignalP 5.0 improves signal peptide predictions using deep neural networks. *Nat. Biotechnol.*, **37**, 420–423 (2019).

20) R. Dustin Schaeffer, Y. Liao, H. Cheng, and N. V. Grishin: ECOD: New developments in the evolutionary classification of domains. *Nucleic Acids Res.*, **45**, D296–D302 (2017).

21) K. Igarashi, T. Ishida, C. Hori, and M. Samejima: Characterization of an endoglucanase belonging to a new subfamily of glycoside hydrolase family 45 of the basidiomycete *Phanerochaete chrysosporium*. *Appl. Environ. Microbiol.*, **74**, 5628–5634 (2008).

22) K. Igarashi, M. Maruyama, A. Nakamura, T. Ishida, M. Wada, and M. Samejima: Degradation of crystalline celluloses by *Phanerochaete chrysosporium* cellobiohydrolase II (Cel6A) heterologously expressed in methylotrophic yeast *Pichia pastoris*. *J. Appl. Glycosci.*, **59**, 105–110 (2012).

23) R. T. DeBoy, E. F. Mongodin, D. E. Fouts, L. E. Tailford, H. Khouri, J. B. Emerson, Y. Mohamoud, K. Watkins, B. Henrissat, H. J. Gilbert, and K. E. Nelson: Insights into plant cell wall degradation from the genome sequence of the soil bacterium *Cellvibrio japonicus*. *J. Bacteriol.*, **190**, 5455–5463 (2008).

24) F. Goubet, C. J. Barton, J. C. Mortimer, X. Yu, Z. Zhang, G. P. Miles, J. Richens, A. H. Liepman, K. Seffen, and P. Dupree: Cell wall glucomannan in Arabidopsis is synthesised by CSLA glycosyltransferases, and influences the progression of embryogenesis. *Plant J.*, **60**, 527–538 (2009).

25) W. Klaudiz: Zur biologisch-mechanischen wirkung der cellulose und hemicellulose im festigungsgewebe der Laubhölzer. *Holzforschung*, **11**, 110–116 (1957).

26) T. Awano, K. Takabe, and M. Fujita: Xylan deposition on secondary wall of *Fagus crenata* fiber. *Protoplasma*, **219**, 106–115 (2002).

27) A. Teleman, J. Lundqvist, F. Tjerneld, H. Stålbrand, and O. Dahlman: Characterization of acetylated 4-O-methylglucuronoxylan isolated from aspen employing ^{1}H and ^{13}C NMR spectroscopy. *Carbohydr. Res.*, **329**, 807–815 (2000).

471 28) D. V. Evtuguin, J. L. Tomás, A. M. S. Silva, and C. P. Neto: Characterization of
472 an acetylated heteroxylan from *Eucalyptus globulus* Labill. *Carbohydr. Res.*,
473 **338**, 597–604 (2003).
474 29) I. Uhliariková, M. Vršanská, B. V. McCleary, and P. Biely: Positional specifity
475 of acetylxylan esterases on natural polysaccharide: an NMR study. *Biochim.*
476 *Biophys. Acta - Gen. Subj.*, **1830**, 3365–3372 (2013).
477 30) R. Naran, S. Black, S. R. Decker, and P. Azadi: Extraction and characterization
478 of native heteroxylans from delignified corn stover and aspen. *Cellulose*, **16**,
479 661–675 (2009).
480 31) P. Naidjonoka, M. A. Hernandez, G. K. Pálsson, F. Heinrich, H. Stålbrand, and
481 T. Nylander: On the interaction of softwood hemicellulose with cellulose
482 surfaces in relation to molecular structure and physicochemical properties of
483 hemicellulose. *Soft Matter*, **16**, 7063–7076 (2020).
484 32) S. Waffenschmidt, and L. Jaenicke: Assay of reducing sugars in the nanomole
485 range with 2, 2′-bicinchoninate. *Anal. Biochem.*, **165**, 337–340 (1987).
486 33) F. Goubet, P. Jackson, M. J. Deery, and P. Dupree: Polysaccharide analysis using
487 carbohydrate gel electrophoresis. A method to study plant cell wall
488 polysaccharides and polysaccharide hydrolases. *Anal. Biochem.*, **300**, 53–68
489 (2002).
490 34) J. R. Bromley, M. Busse-Wicher, T. Tryfona, J. C. Mortimer, Z. Zhang, D. M.
491 Brown, and P. Dupree: GUX1 and GUX2 glucuronyltransferases decorate
492 distinct domains of glucuronoxylan with different substitution patterns. *Plant J.*,
493 **74**, 423–434 (2013).
494 35) D. Floudas, M. Binder, R. Riley, K. Barry, R. A. Blanchette, B. Henrissat, A. T.
495 Martínez, R. Otillar, J. W. Spatafora, J. S. Yadav, A. Aerts, I. Benoit, A. Boyd,

A. Carlson, A. Copeland, P. M. Coutinho, R. P. De Vries, P. Ferreira, K. Findley, *et al.*: The paleozoic origin of enzymatic lignin decomposition reconstructed from 31 fungal genomes. *Science.*, **336**, 1715–1719 (2012).

36) S. C. Potter, A. Luciani, S. R. Eddy, Y. Park, R. Lopez, and R. D. Finn: HMMER web server: 2018 update. *Nucleic Acids Res.*, **46**, W200–W204 (2018).

37) C. Hori, K. Igarashi, A. Katayama, and M. Samejima: Effects of xylan and starch on secretome of the basidiomycete *Phanerochaete chrysosporium* grown on cellulose. *FEMS Microbiol. Lett.*, **321**, 14–23 (2011).

38) K. Sakuragi, C. Hori, K. Igarashi, and M. Samejima: Secretome analysis of the basidiomycete *Phanerochaete chrysosporium* grown on ammonia-treated lignocellulosic biomass from birch wood. *J. Wood Sci.*, **64**, 845–853 (2018).

39) M. H. Johansson, and O. Samuelson: Alkaline destruction of birch xylan in the light of recent investigations of its structure. *Sven. papperstidning*, **80**, 519–524 (1977).

40) P. Biely, C. R. Mackenzie, J. Puls, and H. Schneider: Cooperativity of esterases and xylanases in the enzymatic degradation of acetyl xylan. *Nat Biotechnol*, **4**, 731–733 (1986).

41) M. Busse-Wicher, A. Li, R. L. Silveira, C. S. Pereira, T. Tryfona, T. C. F. Gomes, M. S. Skaf, and P. Dupree: Evolution of xylan substitution patterns in gymnosperms and angiosperms: Implications for xylan interaction with cellulose. *Plant Physiol.*, **171**, 2418–2431 (2016).

42) A. Martínez-Abad, J. Berglund, G. Toriz, P. Gatenholm, G. Henriksson, M. Lindström, J. Wohlert, and F. Vilaplana: Regular motifs in xylan modulate molecular flexibility and interactions with cellulose surfaces. *Plant Physiol.*, **175**, 1579–1592 (2017).

Table 1. Ratios of xylan components.

Xylan components	Free Xyl (%)	GlcA-Xyl (%)	Ac-Xyl (%)	Ara*f*-Xyl (%)
Acetylated xylan from *Arabidopsis thaliana*[6)34)]	34.7[6)34)]	12.1[34)]	53.2[6)]	n.d.
Acetylated xylan from birch wood	45.5 ± 1.2	6.6 ± 0.9	51.1 ± 0.8	n.d.
Acetylated xylan from rice straw	64.5 ± 0.7	0.8 ± 0.1	25.9 ± 0.8	8.7 ± 0.3
Non-acetylated xylan from Japanese cedar	74.8 ± 0.4	17.4 ± 0.2	n.d.	7.8 ± 0.6

The ratio of components of acetylated xylan from *A. thaliana* was taken from the previous reports[6)34)]. Based on NMR spectra data for acetylated xylans from dicots[27)28)29)], acetylated xylans from grasses[7)30)] and non-acetylated xylan from softwood[31)], the peaks were assigned and the ratio of xylan components was estimated from the peak areas. Free Xyl means free xylose residue. GlcA-Xyl, Ac-Xyl and Ara*f*-Xyl mean GlcA-substituted xylose residue, acetylated xylose residue and Ara*f*-substituted xylose residue. n.d. means not detected in this study. Since xylose residues doubly substituted with GlcA and Ac are counted twice, the total is not 100 %.

530 **Table 2.** *S* and τ values and final average DP from time course study.

Enzyme	Substrate	*S* (μM)	τ (h)	Average DP
*Pc*Xyn10A	Acetylated xylan	28.0 ± 0.9	0.21 ± 0.02	9.6
	Deacetylated xylan	47.3 ± 1.2	0.29 ± 0.02	5.8
*Cj*GH10	Acetylated xylan	24.6 ± 1.6	0.12 ± 0.03	11
	Deacetylated xylan	37.4 ± 1.2	0.11 ± 0.01	7.3
*Pc*Xyn11B	Acetylated xylan	5.2 ± 0.8	0.09 ± 0.05	45
	Deacetylated xylan	38.0 ± 2.2	0.34 ± 0.05	7.2
*Np*GH11	Acetylated xylan	7.8 ± 0.2	0.06 ± 0.01	32
	Deacetylated xylan	32.6 ± 0.4	0.05 ± 0.01	8.3

531 Values of *S* and τ were determined based on fitting curves for first-order reaction, as

532 shown in Fig. 2. The average DP after reaction was calculated from the *S* value.

533 **Table 3.** The correlation coefficients between the numbers (left bottom) and the

534 existence (right upper) of GH10, GH11 and CE1 enzymes.

	GH10	GH11	CE1
GH10		0.41	0.39
GH11	0.47		0.62
CE1	0.69	0.72	

535 Data on the numbers and the existence of GH10, GH11 and CE1 enzymes were taken

536 from Floudas *et al*.[35].

Figure legends

Fig. 1. Amino acid sequences of the xylanases.

*Pc*Xyn10A consists of CBM1 (orange) and the GH10 catalytic domain (blue), whereas *Pc*Xyn11B consists of the GH11 catalytic domain (blue) and CBM1 (orange). The red residues are motifs for binding cellulose. CBM1 from *Pc*Xyn10A has a WYY motif while that of *Pc*Xyn11B has a YWY motif.

Fig. 2. Time course study of digestion of acetylated xylan and deacetylated xylan. Reducing ends during the reaction were measured by the BCA method with few modifications. The reaction solution consisted of 4 nM purified enzyme, 1.67 μM acetylated xylan from *A. thaliana*, and 50 mM ammonium acetate buffer (pH 5.0). The same amount of DMSO-extracted xylan was treated with alkali for deacetylation using 4 M NaOH for 20 min and then neutralized by adding 1 M HCl. The ratio of xylan solution, 4 M NaOH and 1 M HCl solution was 200: 5: 20. Curve fitting was performed as described in Materials and Methods section.

Fig. 3. Effect of acetyl groups on degradation of the xylan main chain.

554 A: Separation of oligosaccharides using 10 % PACE gel. The components of the
555 reaction solution were the same as for Fig. 2. The reaction was conducted at 30 ℃ for
556 24 h. Electrophoresis was run at 1,000 V for 45 min. AcXylan and DeAcXylan mean
557 acetylated xylan from *A. thaliana* and deacetylated xylan after alkali treatment. Xyl, X_2,
558 X_3, X_4, X_5 and X_6 are standard xylooligosaccharides: xylose, xylobiose, xylotriose,
559 xylotetraose, xylopentaose and xylohexaose. Stars indicate background bands from
560 substrates. B: Intensity profiles of PACE gels in A analyzed by Image J.
561
562 **Fig. 4.** Comparison of native xylan degradation properties by PACE.
563 A: Comparison of the degradation of various xylans using 10 % PACE gels. AcXylan
564 from BW, AcXylan from RS, Non-AcXylan from JC indicate acetylated xylan from
565 birch wood, acetylated xylan from rice straw and non-acetylated xylan from Japanese
566 cedar. Electrophoresis was run at 1,000 V for 1 h. Acetylated xylans from birch wood
567 and rice straw were extracted by DMSO after delignification. Non-acetylated xylan
568 from Japanese cedar was extracted using 4 M KOH. B: Analysis of gel bands by Image
569 J. The X axis represents the location in the gel and the Y axis represents the intensity of
570 each band.

571 **Fig. 5.** Fungal phylogenetic tree with the numbers of GH10, GH11 and CE1 enzymes.

572 The fungal phylogenetic tree and the numbers of enzymes are based on a previous

573 report[35]. S, ECM, WR, BR, AP, MP, PP and Y in the Ecology column mean non-wood

574 decaying saprotroph, mycorrhiza, white-rot, brown-rot, animal pathogen/parasite,

575 mycoparasite, plant pathogen and yeast, respectively. Refer to the previous paper[35] for

576 fungal names.

>*Pc*Xyn10A
QSPVWGQCGGIGWTGPTTCTAGNVCQEYSAYYSQCIPASQATSVTSVSTAPNPPPTSHTSTSSAPSGASTSTAKLNTLAKAKGKLYFGT
ATDNGELSDTAYTAILDDNTMFGQITPANSMKWDATEPQQGQFTFSGGDQIANLAKSNGMLLRGHNCVWYNQLPSWVSNGKFTAAQLTS
IIQNHCSTLVTHYKGQVYAWDVVNEPFNDDGSWRTDVFYNTLGTSYVQIALEAARAADPDAKLYINEYNIEYAGAKATSLLNLVKTLKA
ASVPLDGIGFQSHFIVGQVPTGLQSQLTTFAAQGVEVAITELDIRMTLPSTPALLAQQKTDYSNVIKACASVEACVGVTVWDWTDKYSW
VPNTFSGQGAACPWDQNFVRKPAYDGIAIGFGN

>*Pc*Xyn11B
FPFEFHNGTHVFPRQSTPAGTGTNNGFFYSFWTDGGGSVTYNNGPAGEYSVTWSNADNFVAGKGWNPGSAQAISFTANYQPNGNSYLSV
YGWSTNPLVEYYILEDFGTYNPAVSLTHKGTLTSDGATYDVYEGTRVNEPSIQGTATFNQYWSIRSSKRSSGTVTTANHFAAWKQLGLP
LGTFNYQIVATEGYQSSGSSTVTVNPAGGVTSPTAPTGPSSVSTTPSGPSSSPSPVGSCAALYGQCGGQGWTGPTCCSSGTCKFSNNWY
SQCL

Fig. 1.

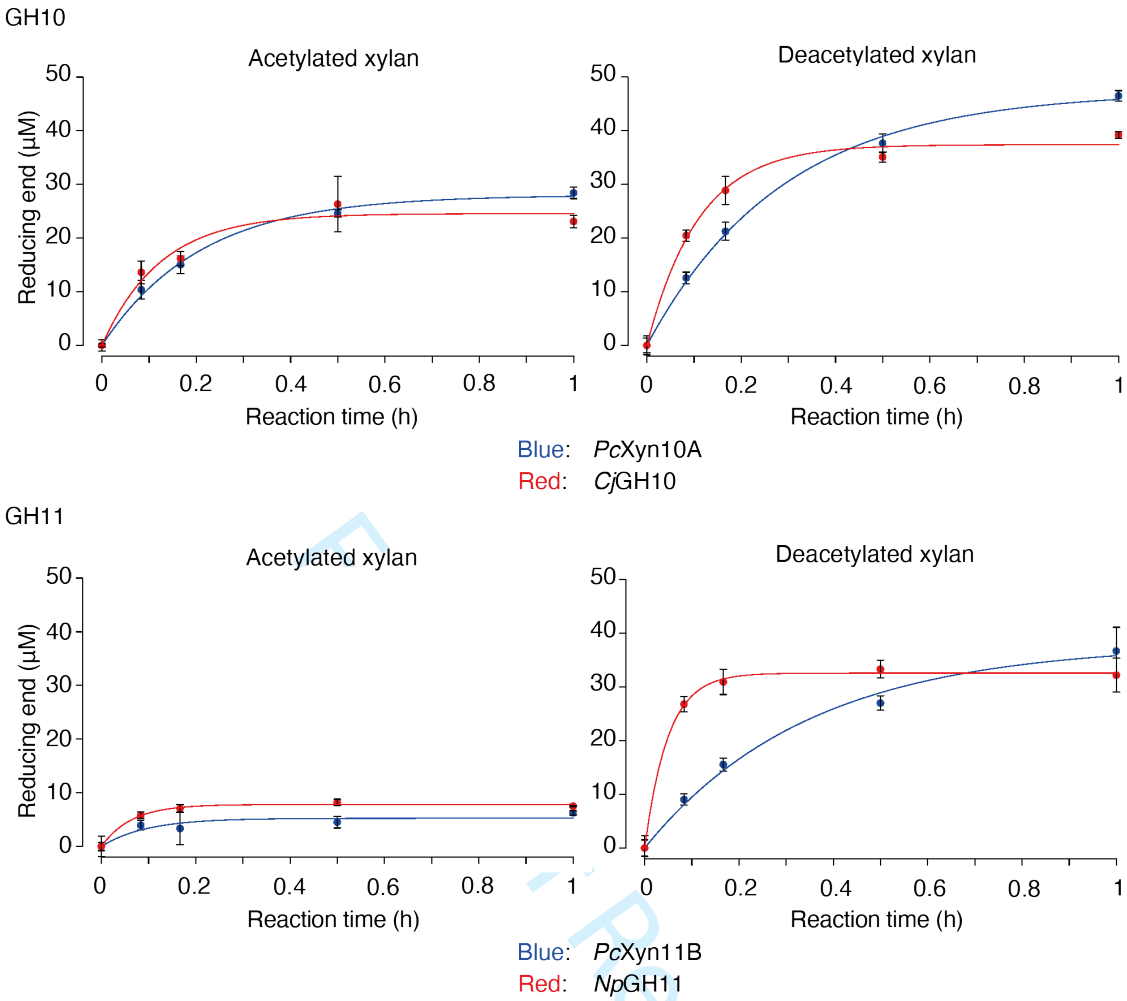

579

580 **Fig. 2.**

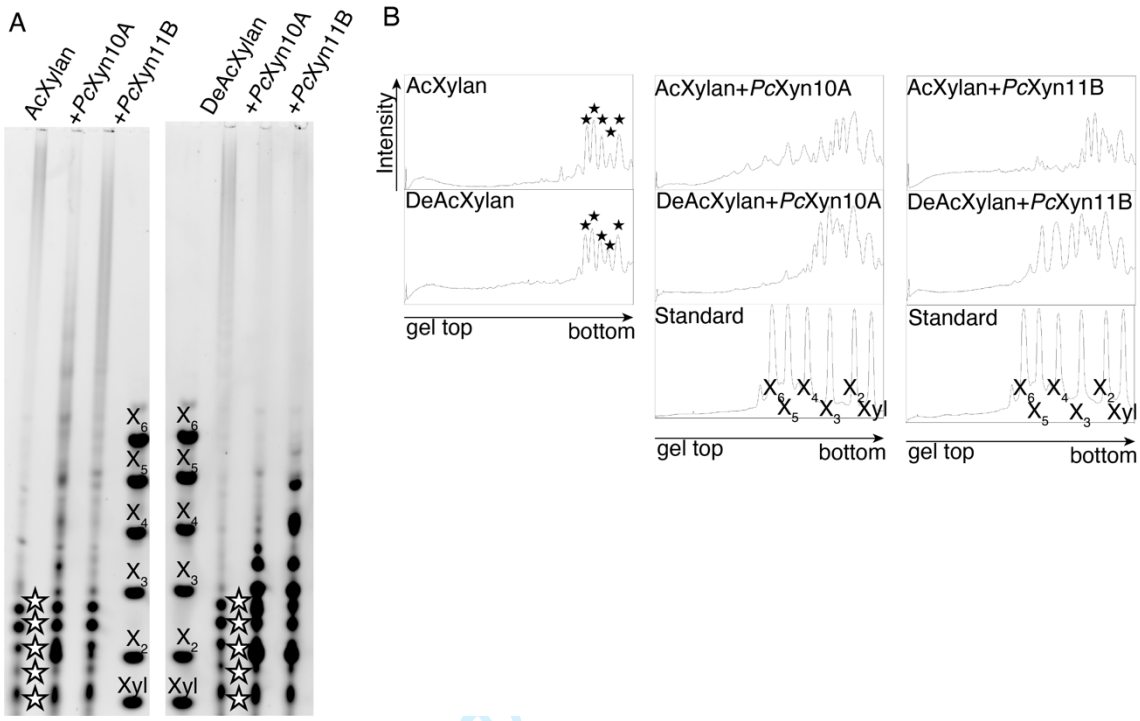

581

582 **Fig. 3.**

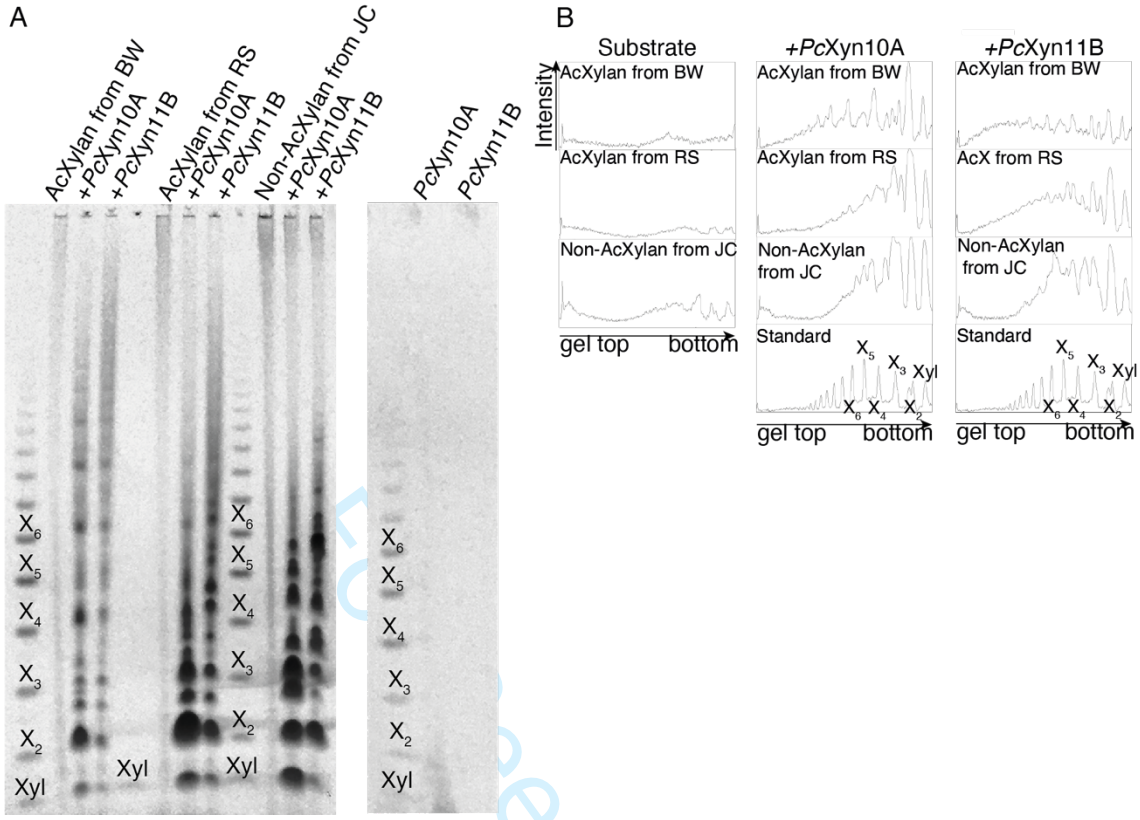

583

584 **Fig. 4.**

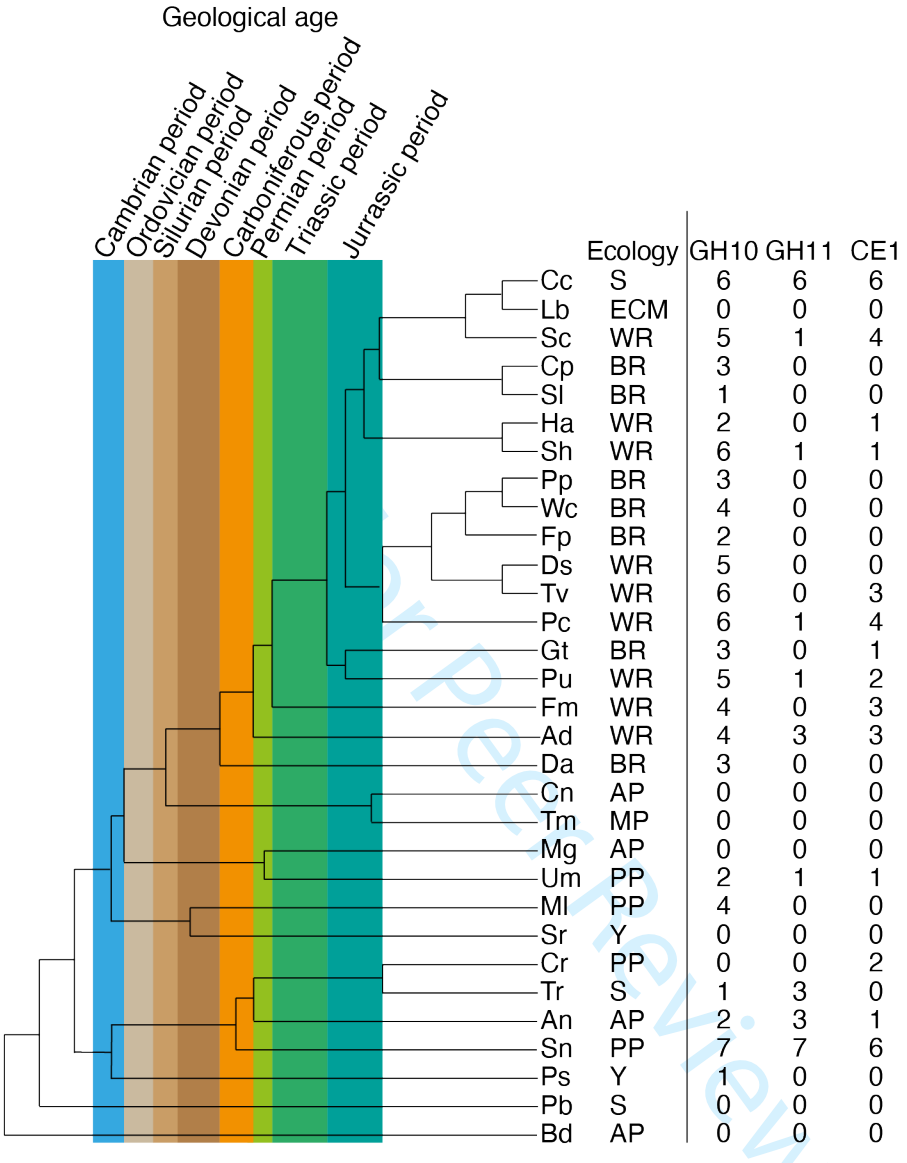

585

586 **Fig. 5.**